GEOPHYSICS, VOL. 43, NO. 1 (FEBRUARY 1978); P. 23–48, 26 FIGS.

MIGRATION BY FOURIER TRANSFORM

R. H. STOLT*

Wave equation migration is known to be simpler in principle when the horizontal coordinate or coordinates are replaced by their Fourier conjugates. Two practical migration schemes utilizing this concept are developed in this paper. One scheme extends the Claerbout finite difference method, greatly reducing dispersion problems usually associated with this method at higher dips and frequencies. The second scheme effects a Fourier transform in both space and time; by using the full scalar wave equation in the conjugate space, the method eliminates (up to the aliasing frequency) dispersion altogether. The second method in particular appears adaptable to three-dimensional migration and migration before stack.

INTRODUCTION

The migration of seismic data has been improved in recent years by application of the theory of scalar waves. Both the difference equation techniques pioneered by Jon Claerbout (1971, 1972, 1976) and integral equation techniques such as those developed by William French (1974, 1975) have been successful as applied.

Described below are two new schemes for the migration of seismic data. Both operate in momentum (i.e., wavenumber or spatial frequency) space in the horizontal (basement) direction. The first scheme is a high-accuracy, high-frequency, steep dip extension of the Claerbout finite difference algorithm. By formulating this algorithm in momentum space, we are able to (a) eliminate a matrix inversion without loss of accuracy, (b) migrate separately each momentum component using an algorithm tailor-made for each, so as to (c) reduce dispersion (within sampling limitations) to negligible proportions.

The second scheme is also based on the scalar wave equation but does not employ finite differences; rather, the exact wave equation is used to predict a transformation in frequency-momentum space. Subject to the sampling limitations of the data, dips of any angle can be migrated correctly and without dispersion.

Emphasis will be placed on digital migration of stacked seismic cross-sections. In addition, the second scheme will be shown to be adaptable to migration before stack and three-dimensional migration.

THEORETICAL FRAMEWORK

General

In what follows, we consider the earth to be a two-dimensional half-space. We assume sound to travel as a scalar field with velocity at point (x, z) of $c(x, z)$. Every point in the earth has the ability to transform downgoing sound waves into upgoing sound waves. This property is characterized by a reflection strength $R(x, z)$ whose angular dependence we ignore. Multiple reflections are also ignored.

Measurements are taken at the earth's surface by placing a source at point (x_s, z_s) and a receiver at (x_0, z_0). The reflected sound wave[1] observed at (x_0, z_0) is represented by $\psi(x_s, z_s, x_0, z_0, t)$, where

[1] ψ may represent a pressure, a displacement or velocity potential, or some other suitably defined parameter. Spatial derivatives of compressibility and density will be largely ignored in what follows, so the distinctions between the various fields will not be of concern here. ψ may be thought of as an impulse response or Green's function.

Manuscript received by the Editor September 8, 1976; revised manuscript received September 30, 1977.
*Continental Oil Co., Ponca City, OK 74601.
0016-8033/78/0201-0023 $0X.00.

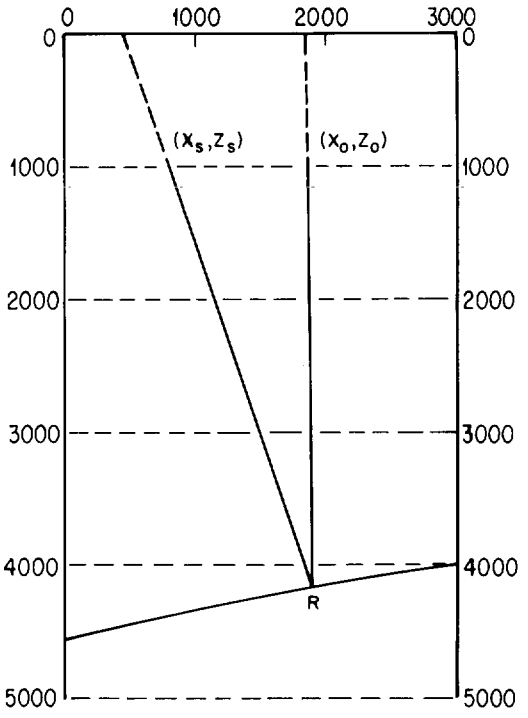

FIG. 1. Migration may be viewed as a prediction of changes in the seismic field as sources and receivers are moved into the earth.

t is the two-way traveltime from source to receiver. For a flat earth, z_s and z_0 are zero during the measurement.

By migration, one attempts to determine the reflection strength $R(x, z)$ from $\psi(x_s, 0, x_0, 0, t)$ at the earth's surface. This is done by predicting what ψ would be for sources and receivers inside the earth. Then (Claerbout, 1971),

$$R(x, z) \sim \psi(x, z, x, z, 0). \tag{1}$$

That is, (x_s, z_s) and (x_0, z_0) are extrapolated to the common point (x, z) as shown in Figure 1. As they approach each other, the traveltime between source and receiver approaches zero, and ψ, subject to limitations in source bandwidth, becomes proportional to the reflection strength at that point.

The changes in ψ as source and receiver migrate into the earth can be predicted by the scalar wave equation. We require (using subscripts to denote partial derivatives),

$$\psi_{x_s x_s} + \psi_{z_s z_s} - \psi_{tt}/c(x_s, z_s)^2 = 0, \tag{2}$$

and

$$\psi_{x_0 x_0} + \psi_{z_0 z_0} - \psi_{tt}/c(x_0, z_0)^2 = 0, \tag{3}$$

at all points in space-time. That is, the scalar wave equation governs ψ with respect to small changes in receiver *or* source location.

Migration of stacked sections

These two equations can be simplified considerably for the migration of stacked sections, if we pretend that "stacked" sections are equivalent to normal incidence sections, where $(x_s, z_s) = (x_0, z_0)$. We define midpoint coordinates,

$$X = (x_s + x_0)/2 \text{ and } Z = (z_s + z_0)/2, \tag{4}$$

and relative, or offset, coordinates,

$$x = (x_0 - x_s)/2 \text{ and } z = (z_0 - z_s)/2. \tag{5}$$

Setting $\psi(X, x, Z, z, t) = \psi(x_s, z_s, x_0, z_0, t)$, the stacked section in the new coordinate system corresponds to $\psi(X, 0, 0, 0, t)$ and the migrated section to $\psi(X, 0, Z, 0, 0)$. Equations (2) and (3) become

$$\psi_{XX} + \psi_{ZZ} + \psi_{xx} + \psi_{zz} - 2\psi_{xX} - 2\psi_{zZ} - 4/c(X - x, Z - z)^2 \psi_{tt} = 0, \tag{6}$$

$$\psi_{XX} + \psi_{ZZ} + \psi_{xx} + \psi_{zz} + 2\psi_{xX} + 2\psi_{zZ} - 4/c(X + x, Z + z)^2 \psi_{tt} = 0.$$

If we ignore derivatives with respect to x and z,[2] we are left with the single equation

$$\psi_{XX} + \psi_{ZZ} - 4/c(X, Z)^2 \psi_{tt} = 0. \tag{8}$$

Equation (8) differs from (2) and (3) by the factor of 4 in the ψ_{tt} term. This difference is due to the fact that in (8), both source and receiver coordinates are required to migrate synchronously, whereas in (2) and (3), one set of coordinates is kept fixed. The form of (8) can be made identical to (2) and (3) by redefining t in (8) to be one-way traveltime.

The Claerbout coordinate transformation

In the Claerbout approach, the wave equation (8) is converted to a difference equation which can be

[2]Strictly speaking, this is hard to justify, though we can argue that as x, $z \to 0$, first derivatives with respect to x and z should vanish, and second derivatives are moveout generators which produce mainly gradual changes of amplitude with time when x and z are fixed at zero.

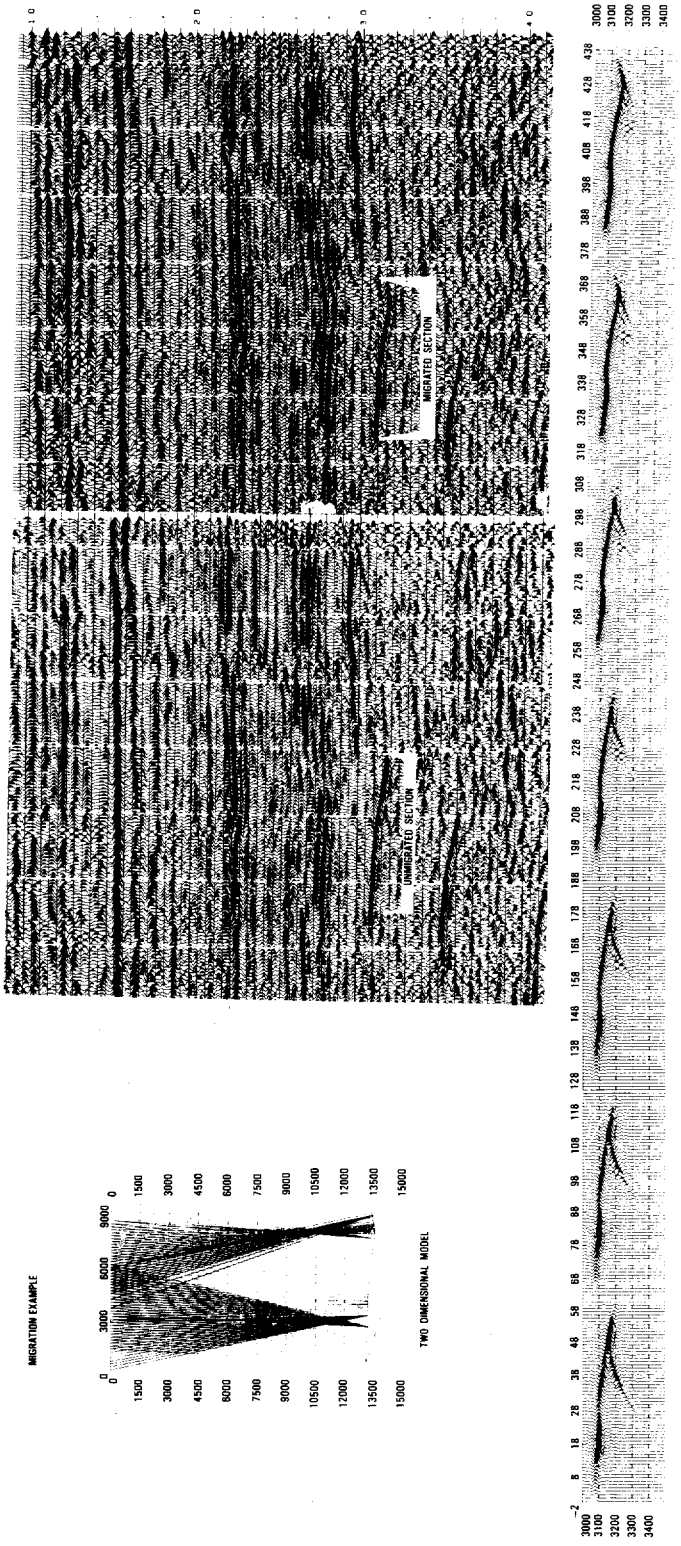

FIG. 2. Migration with an explicit 15 degree finite difference scheme. An inconspicuous event beneath a reflector changes dip direction.

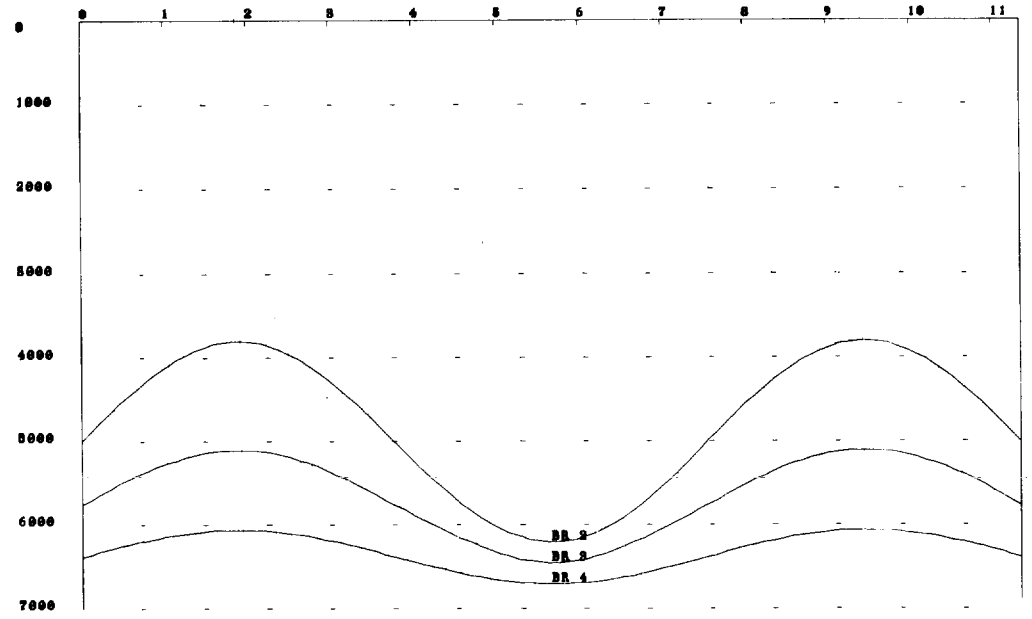

FIG. 3. A two-dimensional earth model. Velocity is 9600 fps in all layers.

used to gradually sink the source-receiver midpoint coordinates (X, Z) into the earth. To make such a scheme practical, Claerbout defines a new coordinate system in which ψ varies less rapidly with depth. If c were constant, one such transformation would be

$$D = ct/2 + Z;\ d = Z. \tag{9}$$

In this coordinate system, D is the depth of some reflection point, while d is the depth of the source-receiver midpoint.

Setting

$$\phi(x, d, D) = \psi(X, 0, Z, 0, t), \tag{10}$$

the wave equation (8) becomes (Claerbout, 1976, p. 211)

$$\phi_{XX} + \phi_{dd} + 2\phi_{dD} = 0. \tag{11}$$

The stacked section corresponds to

$$\begin{aligned}\phi(X, 0, D) &= \phi(X, 0, ct/2) \\ &= \psi(X, 0, 0, 0, t),\end{aligned} \tag{12}$$

and the migrated section to

$$\begin{aligned}\phi(X, D, D) &= \phi(X, Z, Z) \\ &= \psi(X, 0, Z, 0, 0).\end{aligned} \tag{13}$$

Of course, c will normally be a function of X and Z.

A coordinate system which casts the migration problem into a velocity independent form similar to that in equations (11)–(13) will be discussed later.

To help understand equation (11), consider a plane wave of angular frequency $\omega = 2\pi f$ traveling upward at angle θ to the vertical. According to equation (8), such a wave will take the form

$$\psi = e^{i2\omega(X \sin\theta - Z\cos\theta - ct/2)/c}, \tag{14}$$

or, in the new coordinate system,

$$\phi = e^{i2\omega(X\sin\theta + d(1-\cos\theta) - D)/c}. \tag{15}$$

From (15) it follows that for upward traveling waves ϕ_{XX} is always greater than ϕ_{dd}. For waves traveling near the vertical, ϕ_{dd} will be negligible compared to ϕ_{XX}.

THE CLAERBOUT FINITE DIFFERENCE METHOD

Following Claerbout's approach, we now convert the wave equation (11) into a difference equation. Since $\phi_d(X, 0, D)$ is not known a priori, the equation should not involve second differences in d. Since ϕ_{dd} is very small for waves traveling near the vertical, the simplest thing to do is ignore it. This results in the so-called 15 degree approximation to the wave equation (Claerbout, 1976, p. 211)

$$\phi_{XX} + 2\phi_{dD} = 0. \tag{16}$$

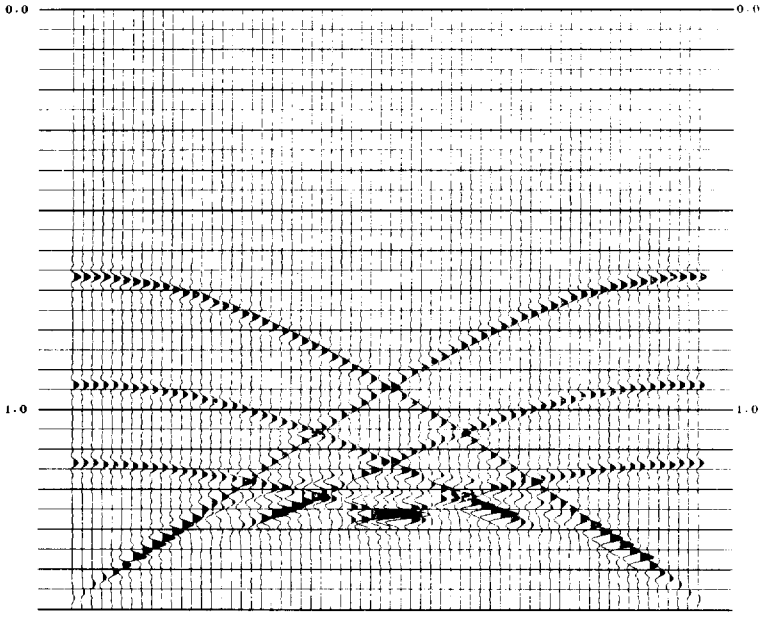

FIG. 4. A synthetic seismic section. Trace spacing is 120 ft.

We now define the discrete variables j and k by the relations

$$D_j = j\Delta D \text{ and } d_k = k\Delta d, \tag{17}$$

where ΔD and Δd are the increments in reflector depth (transformed traveltime) and source-receiver depth, respectively. We also adapt the shorthand notation

$$\phi(X)_j^k \equiv \phi(x, d_k, D_j). \tag{18}$$

The conversion of Equation (16) to a difference equation is not unique. Two possible lowest-order forms are

$$(1 - T)\,\phi_j^{k+1} = -(1 - T)\,\phi_{j+1}^k + (1 + T)(\phi_{j+1}^{k+1} + \phi_j^k), \tag{19a}$$

and

$$\phi_j^{k+1} = -\phi_{j+1}^k + (1 + 2T)(\phi_{j+1}^{k+1} + \phi_j^k), \tag{19b}$$

where

$$T = \frac{\Delta D \Delta d}{8} \frac{d^2}{dX^2}, \tag{20}$$

is an operator in X. In practice, T may be a second (or higher) difference operator in X. The form (19a) is referred to as an implicit solution for ϕ_j^{k+1}, since in order to solve for that quantity, it is necessary to invert the operator $1 - T$. Since no inversion is required in (19b), we call it an explicit solution for ϕ_j^{k+1}.

The implicit form (19a) is a more expensive algorithm than (19b) but has the capacity for greater accuracy at steep dips.

Under many circumstances, the cheap explicit form (19b) will adequately migrate a stacked section. Figure 2 is an example of such a migration in which an apparent downturn of a surface at a fault is converted into an upturn. Migration of a simple model shows the upturn to have developed from an inconspicuous event beneath the reflector. The event appears less prominent on the actual section. This is partly attributable to interference from another event beneath it and partly to losses of diffractive energy during stack. The migration depth increment Δd used to migrate the model was the equivalent of about 500 msec (that is, six steps were required to migrate an event at 3 sec). The actual section was migrated using a smaller increment.

Figures 3 to 5 provide an example of the limitations of the explicit 15 degree algorithm. Figure 3 shows a two-dimensional model consisting of three reflecting surfaces whose depths vary sinusoidally. The maximum dip of the bottom reflector is 15 degrees; that of the middle, 30 degrees; and that of the top, 45

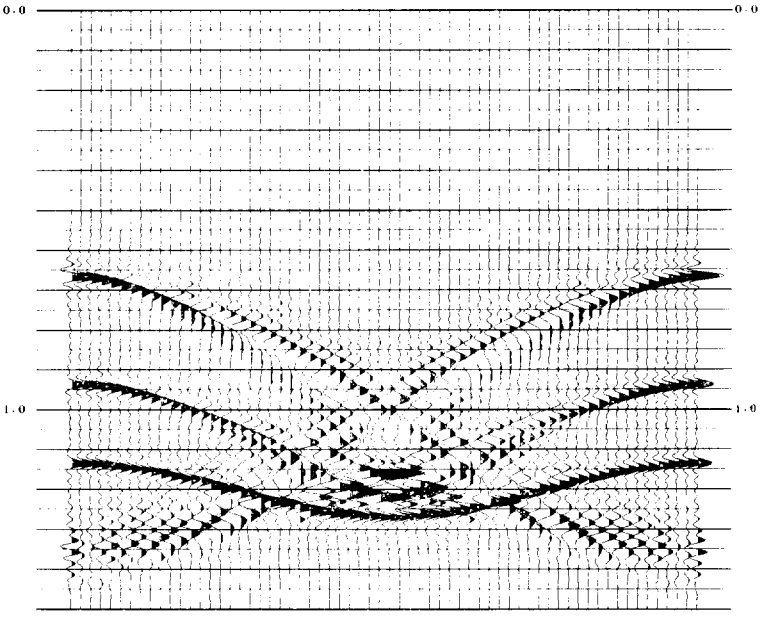

FIG. 5. A 15 degree Claerbout migration (Δd = 860 ft). Note dispersion in regions of steeper dip.

degrees. Velocity is constant at 9600 fps in all layers. Figure 4 is a synthetic normal incidence section constructed from this model, filtered 4–40 Hz. Trace spacing is 120 ft. The 15 degree Claerbout migration of this section is shown in Figure 5. As one might expect, the bottom reflection is migrated properly. The middle reflection, however, shows strong evidence of dispersion (that is, different frequencies are migrated to different places), and the top reflection is less migrated than mangled. Migration step size used was about 860 ft or 180 msec. Use of a smaller Δd step would not, in this case, improve the migration.

Higher order approximations to equation (16) are possible. Little is gained, however, unless the ϕ_{dd} term neglected in (16) is included.

MOMENTUM OR K-SPACE MIGRATION

For waves traveling at large angles to the vertical, ϕ_{dd} (though still smaller than ϕ_{XX}) is not negligible. Since it is not desirable to include ϕ_{dd} explicitly, an approximation must be found.

It is convenient to take a Fourier transform of ϕ with respect to X at this point, defining $p = 2\pi K$ to be the Fourier conjugate of X. Though not necessary for the development of a higher order approximation, there are several advantages to this step. First, the computer time disadvantage of an implicit solution to the wave equation disappears, since the operator inversion becomes a simple division in the wavenumber domain. Second, a simpler algorithm is allowed because the wave equation does not mix traces with different p values. Third, each p value can be migrated separately, using an algorithm individually tailored to it. Finally, the second derivative ϕ_{xx} is well approximated clear up to the spatial Nyquist frequency.

In the wavenumber domain, equation (11) takes the form

$$p^2 \phi = \phi_{dd} + 2\phi_{dD}. \tag{21}$$

We can approximate the effect of ϕ_{dd} by differentiating equation (21) with respect to D,

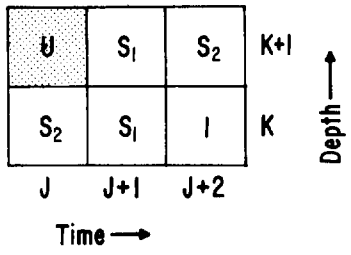

FIG. 6. The two-coeffiecint K-space migration operator.

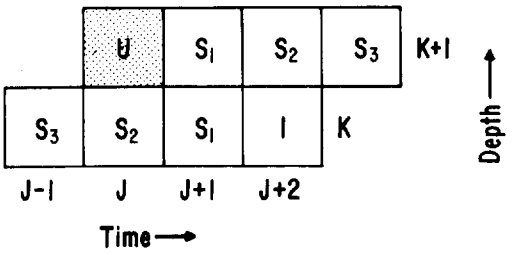

FIG. 7. The three-coefficient K-space migration operator.

$$p^2\phi_D = 2\phi_{dDD} + \phi_{ddD}, \tag{22}$$

and with respect to d:

$$p^2\phi_d = 2\phi_{ddD} + \phi_{ddd}. \tag{23}$$

Neglecting ϕ_{ddd} in (23) allows us to write the single equation,

$$2p^2\phi_D - p^2\phi_d = 4\phi_{dDD}. \tag{24}$$

Equation (24) represents what is commonly called a 45 degree approximation to the scalar wave equation (22).

A simple difference approximation to equation (24) is easily made. Using the discretization formula (18), define the following lowest-order difference operators centered at $(j+1,\ k+1/2)$,

$$\frac{1}{4\Delta D}\left(\phi_{j+2}^{k+1} + \phi_{j+2}^{k} - \phi_{j}^{k+1} - \phi_{j}^{k}\right) \sim \phi_D, \tag{25}$$

$$\frac{1}{\Delta d}\left(\phi_{j+1}^{k+1} - \phi_{j+1}^{k}\right) \sim \phi_d, \tag{26}$$

$$\frac{2}{\Delta d(\Delta D)^2}\left(\phi_{j+2}^{k+1} - \phi_{j+1}^{k+1} + \phi_{j+1}^{k} - \phi_{j}^{k}\right) \sim \phi_{dDD} + \frac{4}{\Delta d \Delta D}\phi_D. \tag{27}$$

Substitution of (25), (26), and (27) into (24) yields the difference equation

$$\phi_j^{k+1} - \phi_{j+2}^{k} + S_1(\phi_{j+1}^{k+1} - \phi_{j+1}^{k}) + S_2(\phi_{j+2}^{k+1} - \phi_j^k) = 0, \tag{28}$$

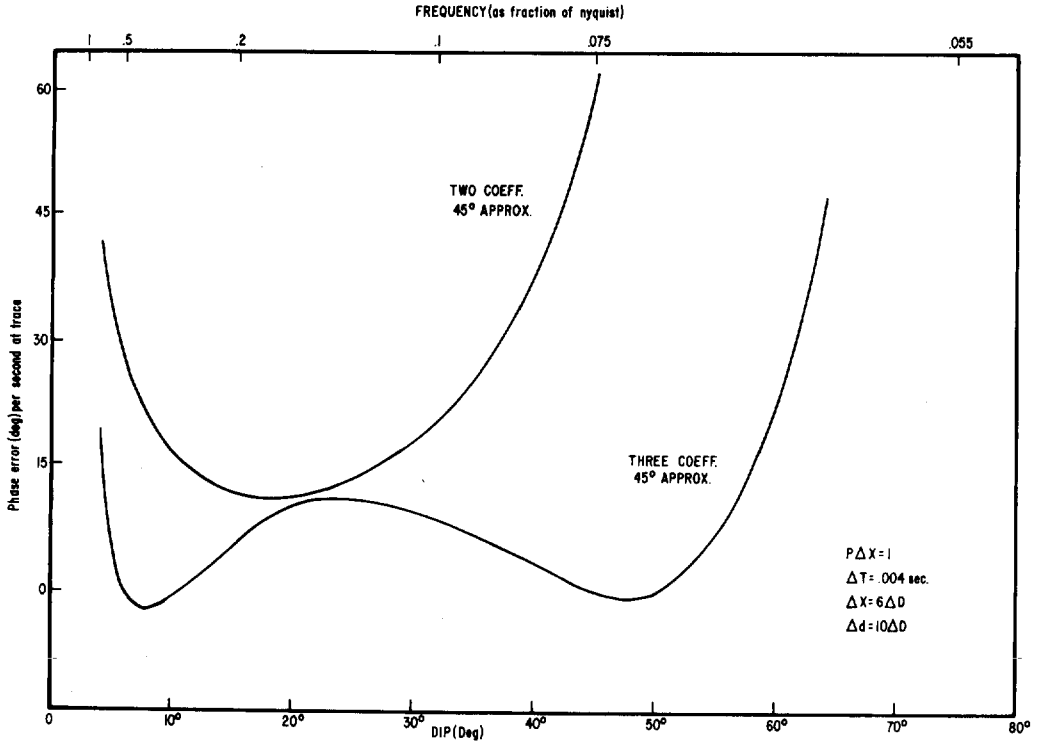

FIG. 8. An illustration of the phase error to be expected from the K-space algorithms.

$$S_1 = -2(8 - p^2\Delta D^2)/(8 + p^2\Delta D\Delta d), \tag{29}$$

$$S_2 = (8 - p^2\Delta D\,\Delta d)/(8 + p^2\Delta D\,\Delta d). \tag{30}$$

Equation (28) allows solution for an unknown ϕ_j^{k+1} in terms of the five known ϕ values illustrated in Figure 6. Stability is assured provided the polynomial,

$$1 + S_1Z + S_2Z^2,$$

has no roots inside the unit circle; i.e., provided its Levinson reflection coefficients (Claerbout, 1976, p. 55–57) are less than one in magnitude. This imposes the constraints

$$|S_2| < 1, \tag{31}$$

and

$$|S_1| < |1 + S_2|, \tag{32}$$

which are automatically met for any migration step size Δd larger than ΔD.

Since X is generally poorly sampled compared to D, and since equation (28) incorporates an extremely accurate approximation to ϕ_{xx}, it might be thought that equation (28) as it stands is an accurate approximation to the wave equation. Unfortunately, that is not the case, the reason being that the low-order approximations to ϕ_D and ϕ_{dDD} have retained errors of the same magnitude as those which were eliminated.

Conversion of (28) to a high accuracy equation is accomplished in two steps. First, we bring in more points along the D-axis. We write,

$$\phi_j^{k+1} - \phi_{j+2}^k + S_1(\phi_{j+1}^{k+1} - \phi_{j+1}^k) + S_2(\phi_{j+2}^{k+1} - \phi_j^k) + S_3(\phi_{j+3}^{k+1} - \phi_{j-1}^k) = 0. \tag{33}$$

That is, the unknown point ϕ_j^{k+1} is determined from the seven points illustrated in Figure 7. Stability is assured provided the polynomial,

$$1 + S_1Z + S_2Z^2 + S_3Z^3,$$

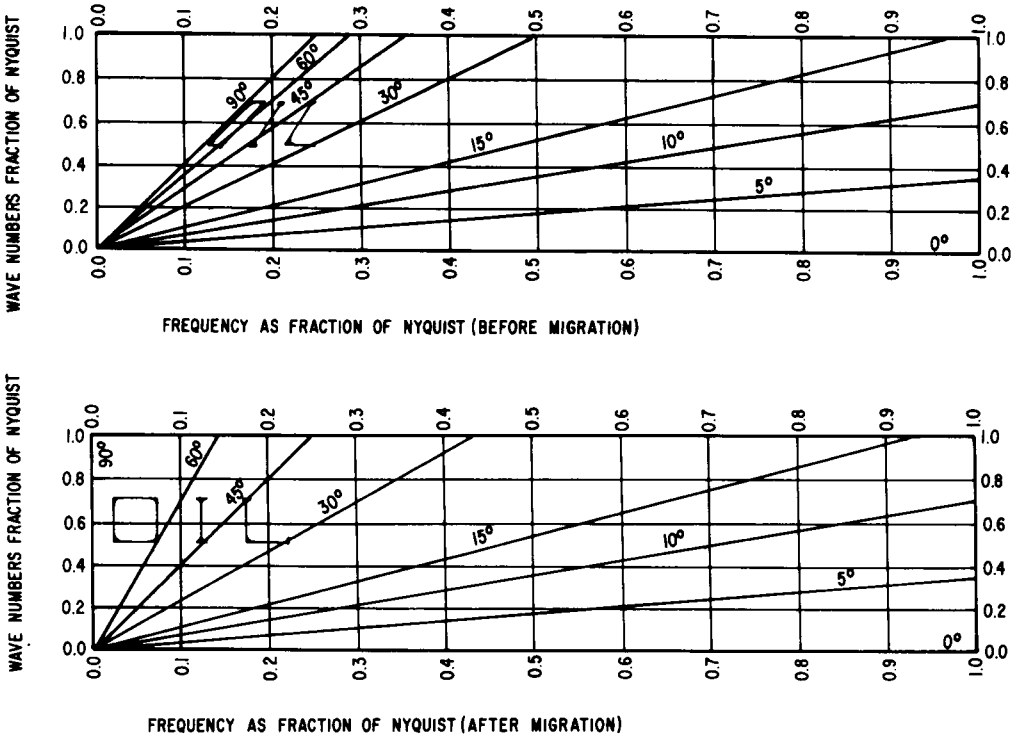

FIG. 9. Migration in *F-K* space.

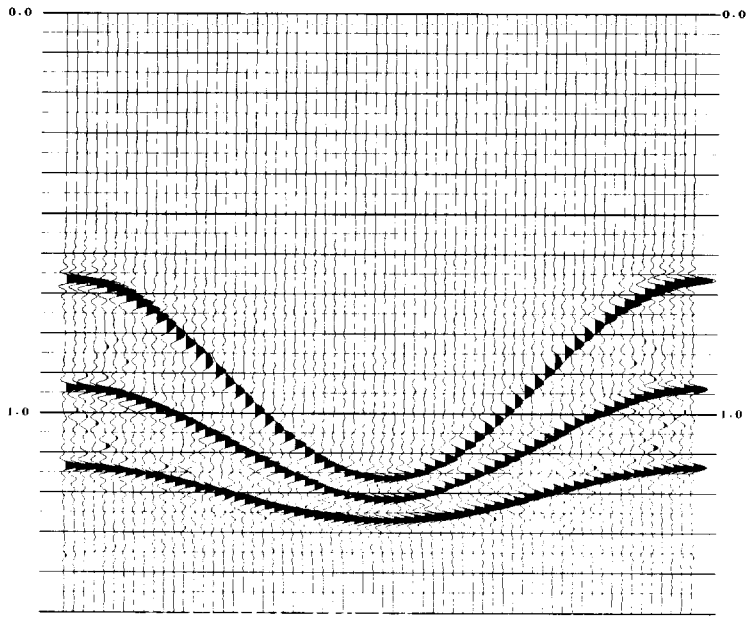

FIG. 10. Migration of a synthetic section using the 45 degree Claerbout algorithm. Maximum phase error is less than 8 degrees for frequencies below the aliasing frequency.

has no roots inside the unit circle. Constraining the Levinson reflection coefficients to be less than one in magnitude, we find

$$|S_3| < 1, \tag{34}$$

$$|S_2 - S_1 S_3| < |1 - S_3^2|, \tag{35}$$

and

$$|S_1 - S_2 S_3| < |1 - S_3^2 + S_2 - S_1 S_3|. \tag{36}$$

The appearance of the anti-causal term ϕ_{j-1}^{k} in equation (33) may be somewhat disquieting, but is really no cause for alarm. It merely reflects the fact that when dealing with bandlimited data, higher order approximations to D-derivatives at the point $j+1$ will use more points on both sides of $j+1$.

The coefficients S_1, S_2, and S_3 may be determined by choosing higher order analogs to the difference operators (25)–(27). However, greater accuracy may be achieved by choosing S_1, S_2, and S_3 so that the difference equation (33) best approximates the exact wave equation (21) rather than the 45 degree approximation (24).

To do this, we look at individual plane wave solutions to equation (21) setting

$$\phi = e^{i(qd - 2\omega D/c)} \tag{37}$$

Equation (21) then gives the dispersion relation (for upcoming waves)

$$q = \frac{2\omega}{c} - \sqrt{\frac{4\omega^2}{c^2} - p^2}. \tag{38}$$

The difference equation (33), on the other hand, gives the relation

$$\sin\left(\frac{\tilde{q}\Delta d}{2} + \frac{2\omega\Delta D}{c}\right) + S_1 \sin\frac{\tilde{q}\Delta d}{2} + S_2 \sin\left(\frac{\tilde{q}\Delta d}{2} - \frac{2\omega\Delta D}{c}\right) + S_3 \sin\left(\frac{\tilde{q}\Delta D}{2} - \frac{4\omega\Delta D}{c}\right) = 0; \tag{39}$$

or, solving for $\tilde{q}$,

$$\tilde{q} = \frac{2}{\Delta d} \arctan \frac{(S_2 - 1)\sin 2\omega\Delta D/c + S_3 \sin 4\omega\Delta D/c}{S_1 + (S_2 + 1)\cos 2\omega\Delta D/c + S_3 \cos 4\omega\Delta D/c}. \tag{40}$$

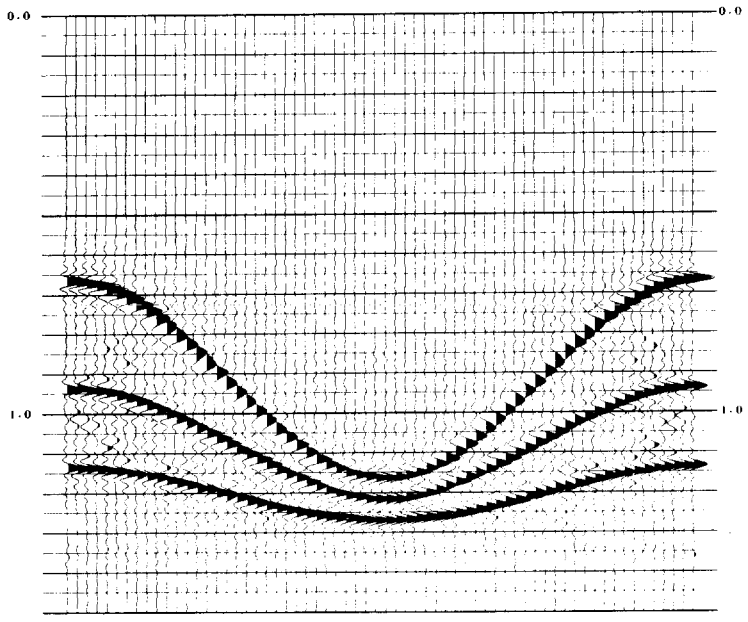

FIG. 11. Migration of a synthetic section using the *F-K* algorithm.

Since $\tilde{q}$ will in general be different from the correct value q, a plane wave of frequency ω and wavenumber p [dip θ = arcsin $(pc/2\omega)$] will develop an error in phase ϵ proportional to the difference $\tilde{q} - q$ and to the distance traveled:

$$\epsilon = (\tilde{q} - q)d. \tag{41}$$

Values for S_1, S_2, and S_3 may be chosen so as to (in some sense) minimize ϵ. ϵ may be forced to zero at any three frequencies by substituting equation (38) into equation (39) and solving the resultant linear set of equations for S_1, S_2, and S_3. Substitution of q at more than three frequencies results in an overdetermined system which can be solved by least squares. If θ_m is the maximum dip present in the data and ω_m the maximum frequency, the frequencies chosen should lie in the range

$$pc/2 \sin \theta_m < \omega < \omega_m. \tag{42}$$

Figure 8 illustrates the phase errors to be expected from the two-coefficient difference equation (28) and the three-coefficient equation (33). In this example, $p\Delta X = 1$ radian, $\Delta X = 6\Delta D$, and $\Delta d = 10\ \Delta D$. For the two-coefficient equation, $S_1 = -1.926174$, $S_2 = .932886$. For the three-coefficient equation, $S_1 = -1.913213$, $S_2 = .914654$, and $S_3 = .010563$. These values were chosen to give zero-phase error at $\omega_1 =$ Nyquist/2, $\omega_3 = pc/2\sin 45$ degrees, and $\omega_2 = (\omega_1 + \omega_3)/2$. Phase error is plotted in degrees per second of trace, assuming a .004 sec sample interval. Two things are apparent in this illustration: (1) equation (33) is more accurate than equation (28) over the entire range of dips and frequencies; and (2) by forcing three zero crossings for equation (33), we have actually gotten four (the fourth zero crossing occurs at about 50 degree dip), significantly extending its region of accuracy. This suggests that (a) modification of the coefficients of equation (28) could not produce accuracy comparable to that of equation (33); and (b) adding a fourth coefficient to equation (33) is not likely to significantly improve accuracy.

In practice, equation (33) is found to be accurate and stable for dips up to 45–55 degrees. Beyond this, accuracy may require an extremely small Δd, and stability problems may be encountered. Note that in general the coefficients S_1, S_2, and S_3 and also the step size Δd will be different for every spatial frequency p.

The phase error defined in equation (41) does not include error introduced by a finite sample interval ΔX in X. In principle, these errors are zero, provided the maximum dip angle $\theta_{\max}$ obeys

$$\theta_{\max} < \text{arc sin } (\Delta D/\Delta X). \tag{43}$$

If the maximum frequency in the data is $f_{\max} = \nu$

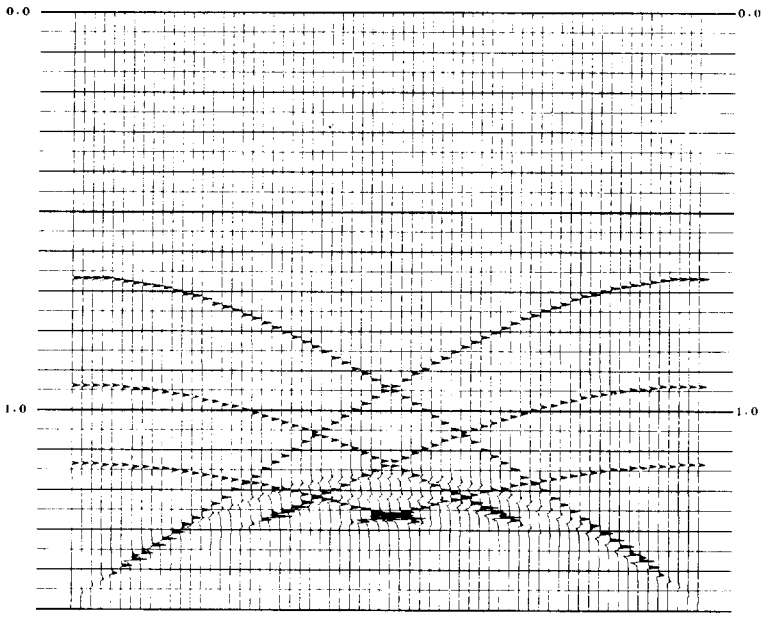

FIG. 12. A synthetic seismic section.

fnyq, where *fnyq* is the Nyquist frequency (125 Hz for $\Delta t = 4$ msec), then the above relation becomes less restrictive:

$$\theta_{\max} < \text{arc sin } (\Delta D / v \Delta X). \tag{44}$$

Dips θ greater than $\theta_{\max}$ are migrated correctly as long as frequency obeys

$$f < fnyq \cdot \Delta D / DX \sin\theta \equiv f_a. \tag{45}$$

f_a will be referred to as the aliasing frequency.

At larger frequencies, the dip will be interpreted as smaller than $\theta_{\max}$ and will be migrated incorrectly.

Examples of migration using the equation (33) algorithm will be deferred until after a discussion of the $F - K$ migration scheme.

MIGRATION IN F–K SPACE

Suppose we take a two-dimensional Fourier transform of the surface field $\phi(X, 0, D)$:

$$A(p, \omega) = \frac{1}{2\pi} \int dX \int dD\, e^{i(pX - 2D/c)} \phi(X, 0, D), \tag{46}$$

so that

$$\phi(X, 0, D) = \frac{1}{2\pi} \int dp \int d\omega e^{-i(pX - 2\omega D/c)} A(p, \omega). \tag{47}$$

For upcoming waves, equation (47) generalizes at positive depth to

$$\phi(X, d, D) = \frac{1}{2\pi} \int dp \int d\omega e^{-i(pX + qd - 2\omega D/c)} A(p, \omega), \tag{48}$$

where, to satisfy the wave equation (11),

$$q = \frac{2\omega}{c} - \sqrt{\frac{4\omega^2}{c^2} - p^2}. \tag{49}$$

The migrated section $\phi(X, D, D)$ then has the form

$$\phi(X, D, D) = \frac{1}{2\pi} \int dp \int d\omega A(p, \omega) e^{-i\left\{pX - \sqrt{\left(\frac{4\omega^2}{c^2} - p^2\right)} D\right\}}. \tag{50}$$

The substance of equations (46) and (50) is that migration may be accomplished by a double Fourier transform of the original data from (X, D) space into (p, ω) space (46), followed by the more complicated transformation (50). If equation (50) could be converted into a double Fourier transform, a practical migration scheme could result.

Fortunately, a simple change of variable from ω to

$$k = \sqrt{\frac{4\omega^2}{c^2} - p^2}$$

does the trick:

$$\phi(X, D, D) = \frac{1}{2\pi} \int dp \int dk\, B(p, k) e^{-i(pX - kD)}, \tag{51}$$

where

$$B(p, k) = \frac{1}{\sqrt{1 + p^2/k^2}} A\left(p, \frac{kc}{2}\sqrt{1 + p^2/k^2}\right). \tag{52}$$

The transformation (52) represents, for a fixed p, a shift of data from frequency ω to a lower frequency $\omega' = \sqrt{\omega^2 - p^2c^2/4}$ (in fact, a "moveout correction" where ω takes the place of time, and p of offset), plus a change of scale $k/\sqrt{k^2 + p^2} = \omega'/\omega$. The frequency shift, depicted in Figure 9, effects only what migrators have always known, namely that an apparent dip of θ_A before migration translates into a dip,

$$\theta_M = \text{arc sin tan } \theta_A, \tag{53}$$

after migration.

The operations (46), (51), and (52) could easily be done in an analog system. On a digital computer, the Fourier transforms (46) and (51) will be carried out as FFTs. The transformation (52) then involves a dangerous interpolation of the data in the frequency domain. To avoid ghost events appearing on the section, it is usually necessary at least to double the trace length by adding zeros before performing the initial time FFT.

No phase error or dispersion should be seen in double Fourier transform migration, since the exact wave equation is used. The aliasing problem discussed in the last section will still be present, though it is now possible to predict exactly where aliasing may exist and conceivably even unravel it.

EXAMPLES OF FOURIER TRANSFORM MIGRATION

Migrations of the synthetic section of Figure 4 are shown in Figures 10 and 11. Figure 10 results from k-space finite difference algorithm (33). Maximum-phase error at the bottom of the section was held to less than 8 degrees. All three reflectors have assumed their proper shapes. Little dispersion is evident, except for a loss of high frequencies in the region of 45 degree dip. This would be expected, since the aliasing frequency at that dip is 28.3 Hz. Figure 11 shows a migration using the double Fourier transform (F-K) algorithm. It appears very similar to the K-space finite difference migration (Figure 10).

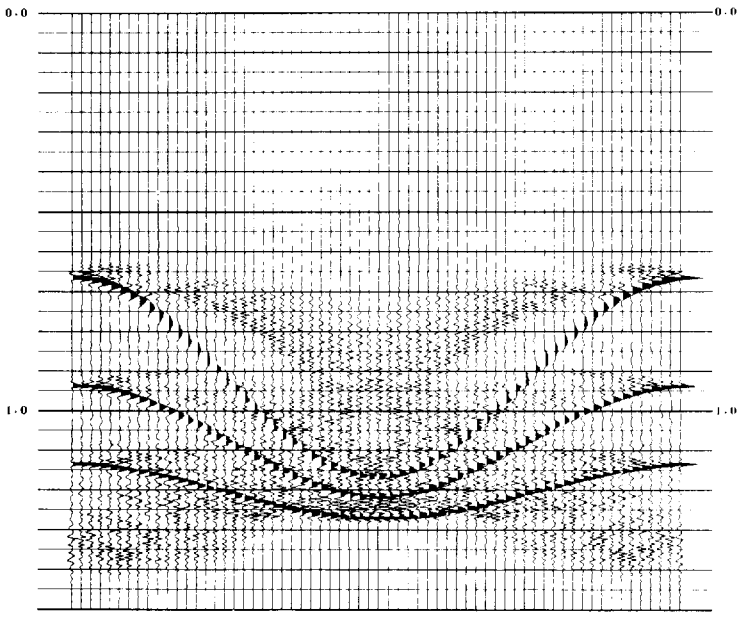

FIG. 13. A K-space migration.

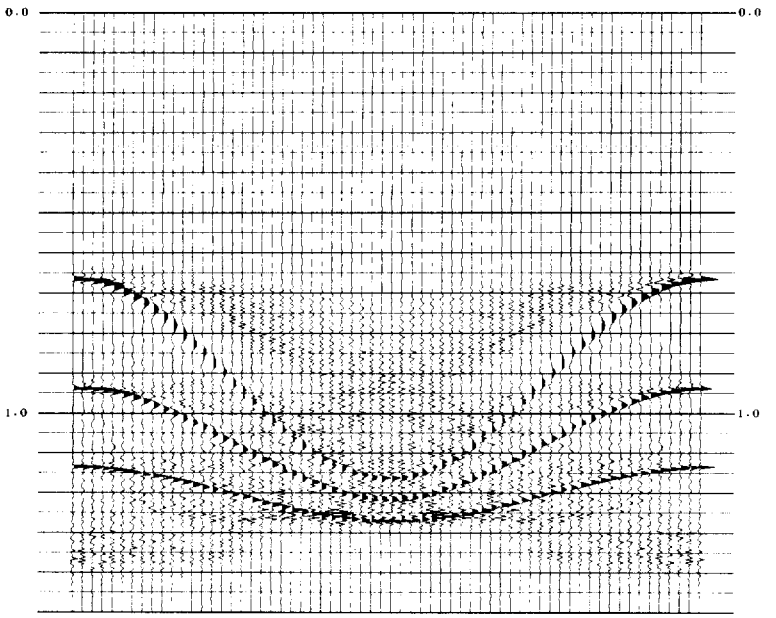

FIG. 14. An *F-K* migration.

Figures 12 to 14 show more clearly what happens to frequencies above the aliasing frequency. Figure 13 shows a *K*-space finite difference migration of the same model as before with a frequency range expanded to 0–90 Hz. Figure 14 is an *F-K* migration in the range 0–125 Hz. The similarity between the two migrations is still apparent. Frequencies below the aliasing frequency are in both cases migrated properly, while frequencies above it are undermigrated, mostly remaining close to their original position.

The remaining examples involve seismic field data. Maximum dip on Figure 15 is of the order of 35 degrees. Trace spacing is 220 ft, with rms velocities ranging from 7000 to 13,000 fps. Figure 16 is the *K*-space finite difference migration (maximum phase error <3 degrees); Figure 17 the *F-K* migration. Though some differences are apparent in the two migrations (due in part to slightly different parameterizations), they give substantively the same reasonable subsurface picture.

Figure 18 is a somewhat more complex section. The 15 degree Claerbout migration, shown in Figure 19, leaves several crossing events and some dispersion. The *K*-space and *F-K* migrations in Figures 20 and 21 give a more satisfying picture with a substantively different interpretation. Residual crossing events indicate a three-dimensional structure.

In Figure 22, the structure is actually three-dimensional, involving dips in excess of 45 degrees. To complicate matters, crucial data from the steep north flank of the structure were not recorded. Trace spacing is 220 ft, with rms velocities in the 7000–14,000 fps range. The *K*-space and *F-K* migrations in Figures 23 and 24 are again very similar. In this case, the results are predictably less than perfect but do provide some basis for interpretation.

The concluding section, Figure 25 is a regional seismic line. Its *F-K* migration, Figure 26, is a dramatic illustration of steep dip migration.

MIGRATION BEFORE STACK

The *F-K* migration scheme in principle can be used to effect moveout correction, stack, and migration of data in one process. In this case, we use a three-dimensional Fourier transform in the coordinate system specified in equations (4) and (5):

$$A(P, p, \omega) = (2\pi)^{-3/2} \int dt \int dX \cdot \cdot \int dx e^{i(PX + px - \omega t)} \psi(X, x, 0, 0, t). \tag{54}$$

We assume the field to be governed by the two wave equations (2) and (3), where, for simplicity, c is assumed constant. Then,

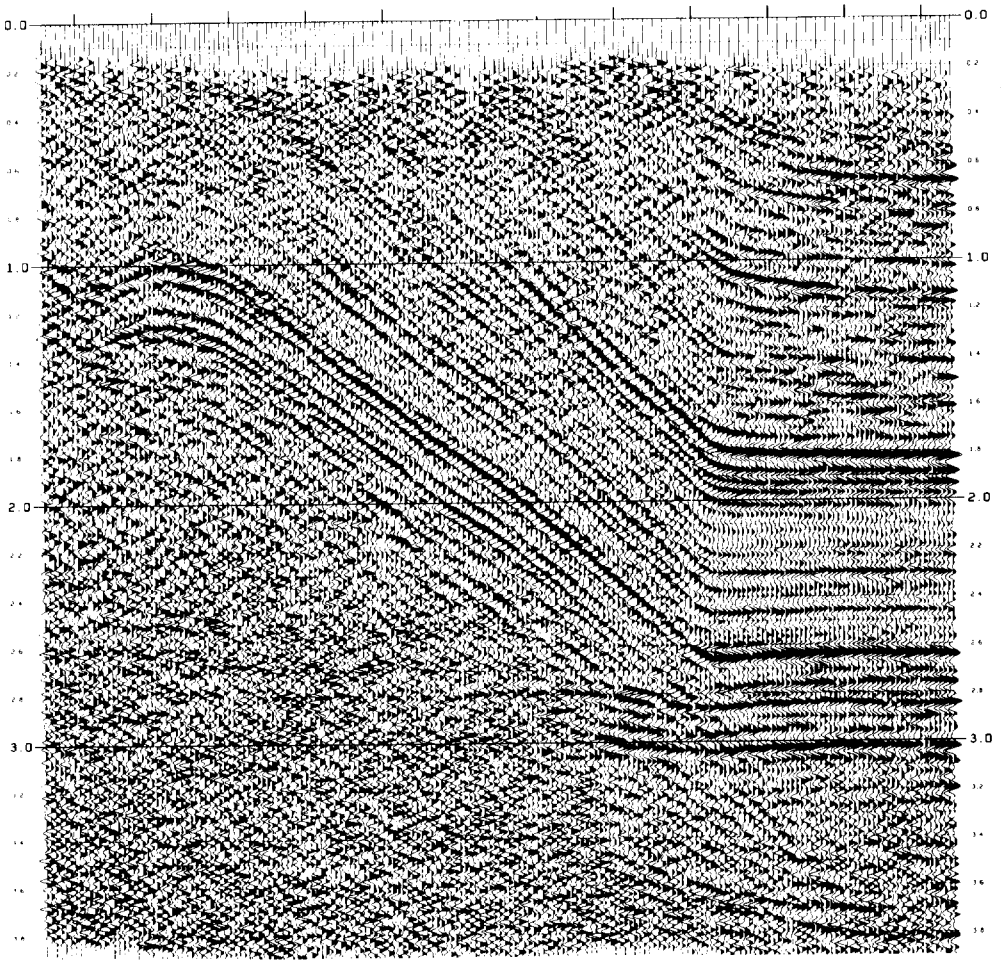

FIG. 15. Five-fold CDP section maximum dip 35 degrees.

$$\psi(X, x, (z_0 + z_s)/2, (z_0 - z_s)/2, t)$$
$$= (2\pi)^{-3/2} \int d\omega \int dP \int dp \cdot$$
$$\cdot e^{-i(PX + px - q_s z_s - q_0 z_0 - \omega t)} A(P, p, \omega), \quad (55)$$

where, from equations (2) and (3)

$$q_s = \omega/c \sqrt{1 - (P - p)^2 c^2/4\omega^2};$$
$$q_0 = \omega/c \sqrt{1 - (P + p)^2 c^2/4\omega^2}. \quad (56)$$

The migrated section is

$$\psi(X, 0, ct/2, 0, 0)$$
$$= (2\pi)^{-3/2} \int d\omega \int dP \cdot$$
$$\cdot \int dp\, e^{-i(PX - (q_s + q_0)ct/2)} A(P, p, \omega). \quad (57)$$

To put (57) in the form of a Fourier transform, a coordinate transformation is required. We define two new variables which will replace p and ω,

$$u = q_s + q_0; \; v = q_s - q_0. \quad (58)$$

From equations (56) and (58) follow the relations,

$$p = uv/P, \quad (59)$$

$$\omega = sgn(\omega)(c/2P)\sqrt{P^4 + P^2(u^2 + v^2) + u^2v^2}, \tag{60}$$

and

$$\psi(X, 0, ct/2, 0, 0) = (2\pi)^{-3/2} \int dP \int du \int dv\, e^{-i(PX - uct/2)} \cdot \cdot A(P, p, \omega)c^2(u^2 - v^2)/4\omega P. \tag{61}$$

Again, a simple transformation accomplishes the migration process. Note that the Fourier p-integral becomes a simple integration over v, since only zero offset is relevant after migration.

MIGRATION IN THREE DIMENSIONS

The three-dimensional analog of equation (8) is

$$\psi_{XX} + \psi_{YY} + \psi_{ZZ} - 4/c^2\, \psi_{tt} = 0. \tag{62}$$

When c is constant, we can write

$$\psi(X, Y, Z, t) = (2\pi)^{-3/2} \int dP\, e^{iPX} \int dQ\, e^{iQY} \cdot \cdot \int d\omega\, e^{-i\omega t} A(P, Q, \omega, Z), \tag{63}$$

where

$$A(P, Q, \omega, 0) = (2\pi)^{-3/2} \int dX \int dY \cdot \cdot \int dt\, \psi(X, Y, 0, t)\, e^{-i(PX + QY - \omega t)}, \tag{64}$$

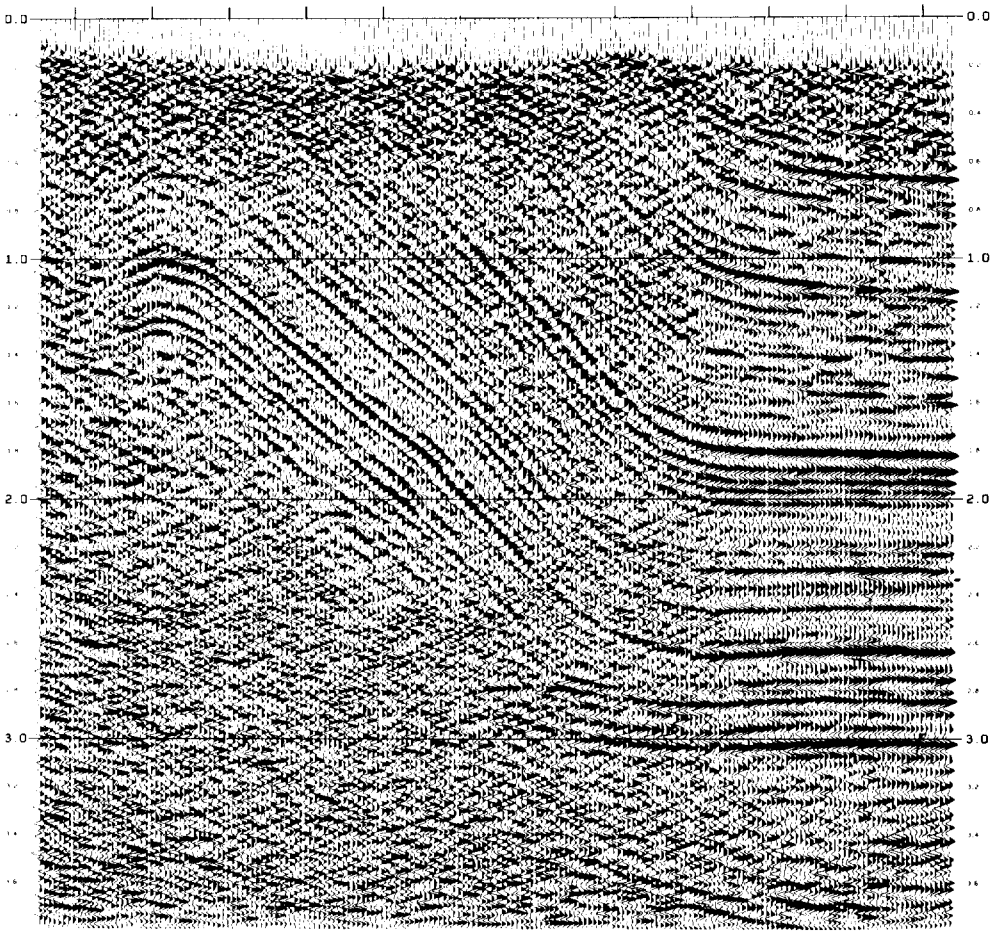

FIG. 16. A K-space migration of Figure 11.

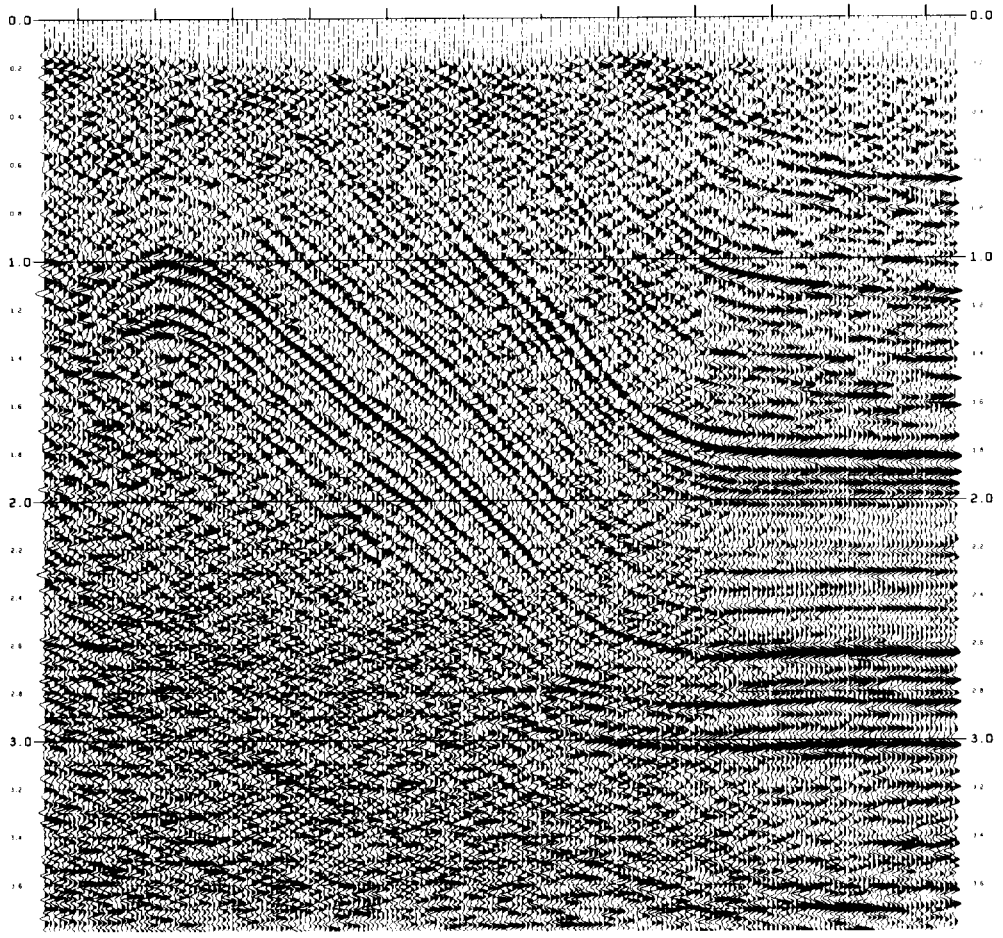

FIG. 17. An *F-K* migration of Figure 11.

is the triple Fourier transform of the unmigrated three-dimensional data. Now, $A(P, Q, \omega, Z)$ satisfies the transformed wave equation

$$A_{ZZ} = (P^2 + Q^2 - 4\omega^2/c^2)A, \tag{65}$$

which has upcoming solutions,

$$A(P, Q, \omega, Z) = A(P, Q, \omega, 0)e^{-iZ\sqrt{4\omega^2/c^2 - P^2 - Q^2}}. \tag{66}$$

EXTENSION TO A VARIABLE VELOCITY

The *K*-space migration scheme described above relies on a velocity which is *X*-independent. The derivation of the *F-K* algorithm was even more restrictive, requiring velocity to be constant. In order to use these schemes in the presence of a variable velocity, it is necessary to transform to a coordinate

Hence, we can write the migrated field as,

$$\psi(X, Y, Z, 0) = (2\pi)^{-3/2} \int dP \int dQ \int d\omega B(P, Q, \omega)e^{i(PX + QY - 2\omega Z/c)}, \tag{67a}$$

where

$$B(P, Q, \omega) = A\{P, Q, \omega\sqrt{1 + (P^2 + Q^2)c^2/4\omega^2}\}/\sqrt{1 + (P^2 + Q^2)c^2/4\omega^2}. \tag{67b}$$

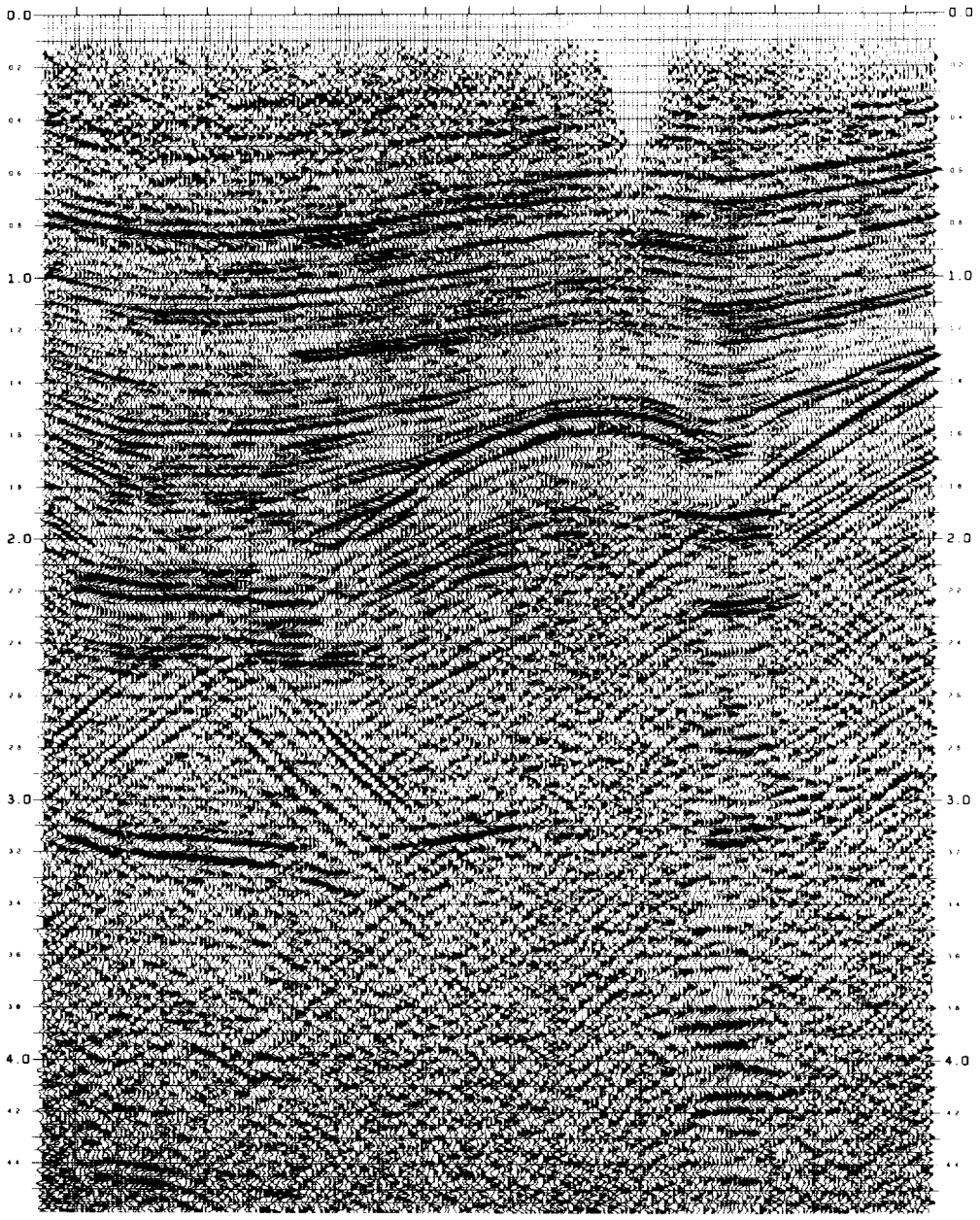

FIG. 18. A complex 10-fold CDP section.

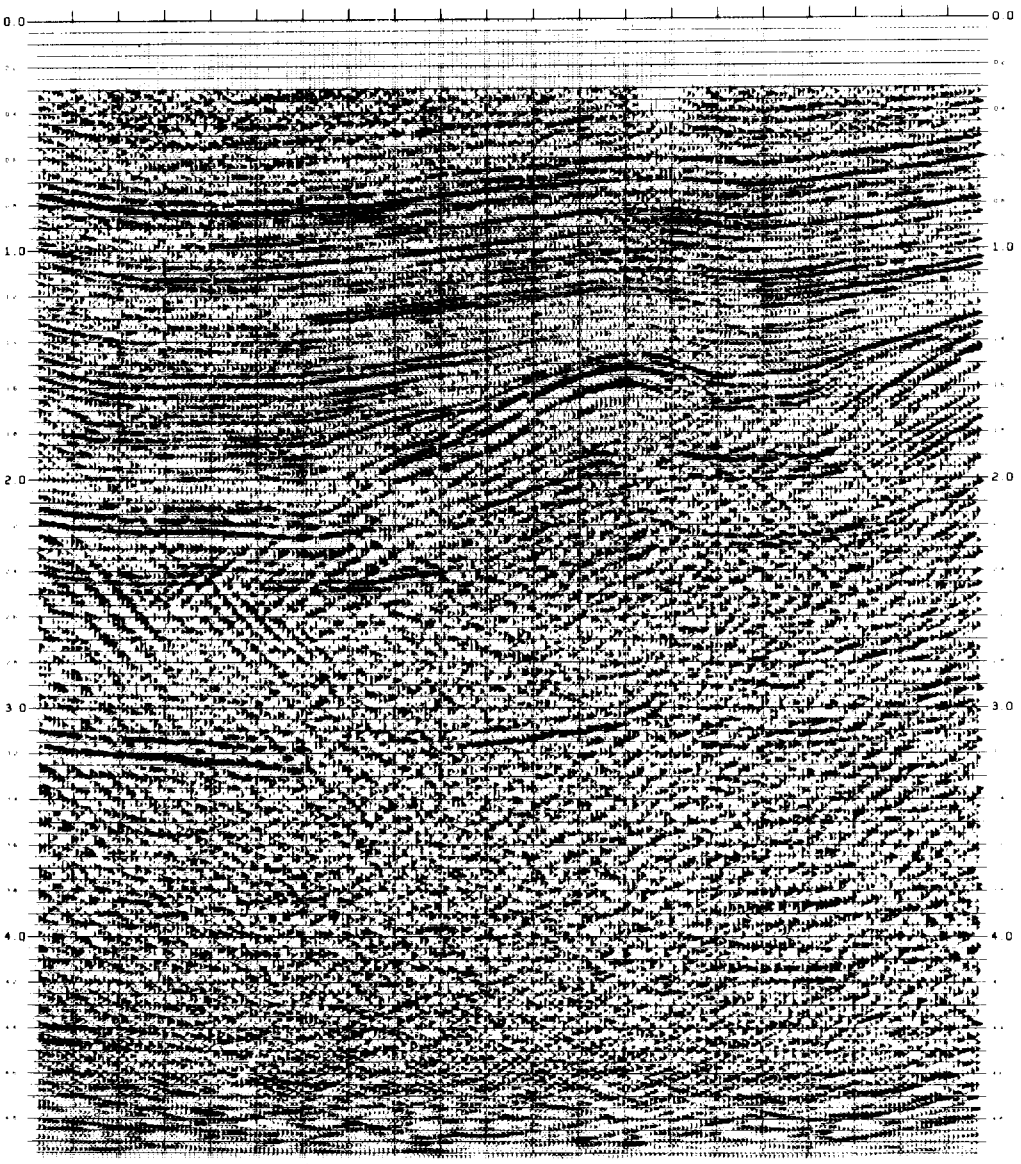

FIG. 19. A 15 degree Claerbout migration of Figure 14.

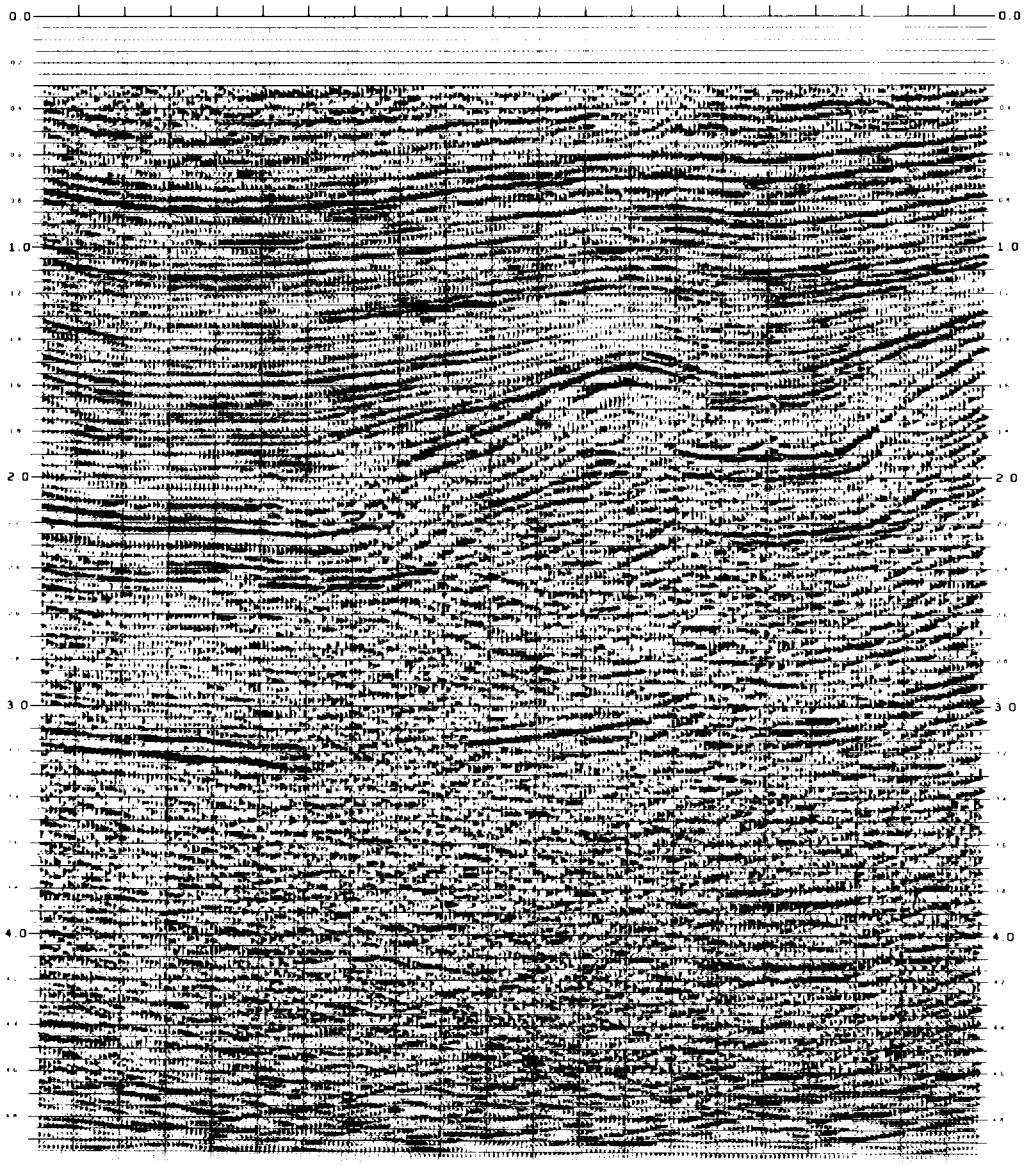

FIG. 20. A K-space migration of Figure 14.

system in which both the wave equation and the boundary conditions are velocity independent.

Beginning with the coordinate system X, Z, t of equation (8), we first define new time and depth coordinates

$$t' = \frac{t}{2} + \int_0^Z \frac{dZ}{c}, \tag{68}$$

$$Z' = \frac{1}{c_0} \int_0^Z dZc. \tag{69}$$

Since Z' represents the apparent depth to a reflector at Z in a layered medium, we may expect this to be a useful coordinate system for migration. Neglecting velocity derivatives, the wave equation becomes

$$\psi'_{XX} + c^2/c_0^2 \psi_{Z'Z'} + 2/c_0 \psi'_{Z't'} = 0. \tag{70}$$

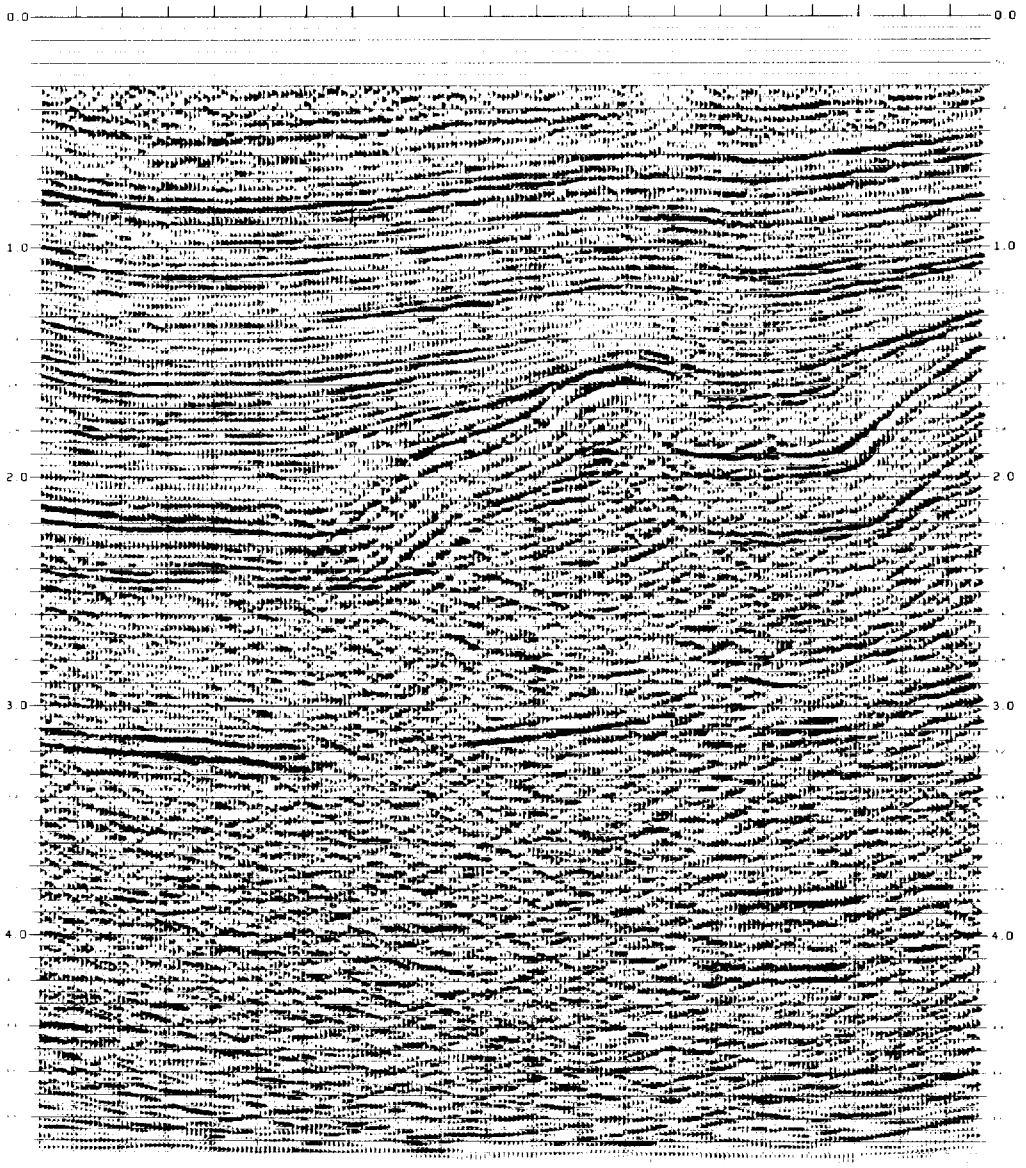

FIG. 21. An *F-K* migration of Figure 14.

Note that the coefficient of the dominant ψ_{Zt} term is now constant. To define the migration limits in this coordinate system, we define two new variables $\zeta(t')$ and $\eta(t')$

$$t' = \int_0^\zeta \frac{dZ}{c}, \tag{71}$$

and

$$\eta = \int_0^\zeta c\, dZ. \tag{72}$$

Then before migration the limits are

$$Z' = 0,\ t' > 0, \tag{73}$$

and the limits upon migration are

$$Z' = \eta(t')/c_0,\ t' > 0. \tag{74}$$

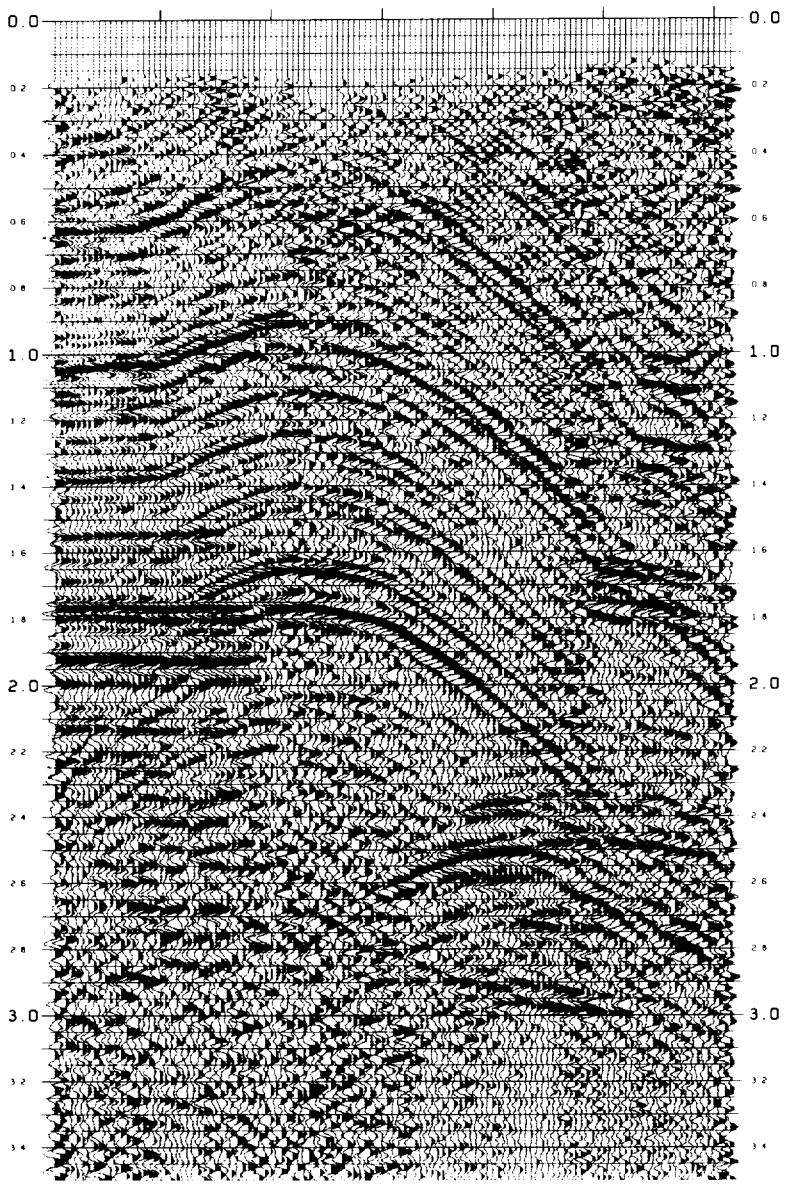

FIG. 22. A 10-fold CDP section with dips greater than 45 degress.

Because Equation (74) is time dependent, this coordinate system is not in general useable for K-space or F-K migration. However, one more change of variables will do the trick. Define

$$D = \sqrt{2 \int_0^{t'} \eta(t')\, dt'} \tag{75}$$

and

$$d = Z' c_0 D / \eta. \tag{76}$$

Setting $\phi(X, d, D) = \psi(X, Z, t)$, the wave equation takes the form

$$\phi_{XX} + W(X, d, D)\, \phi_{dd} + 2\, \phi_{dD} = 0, \tag{77}$$

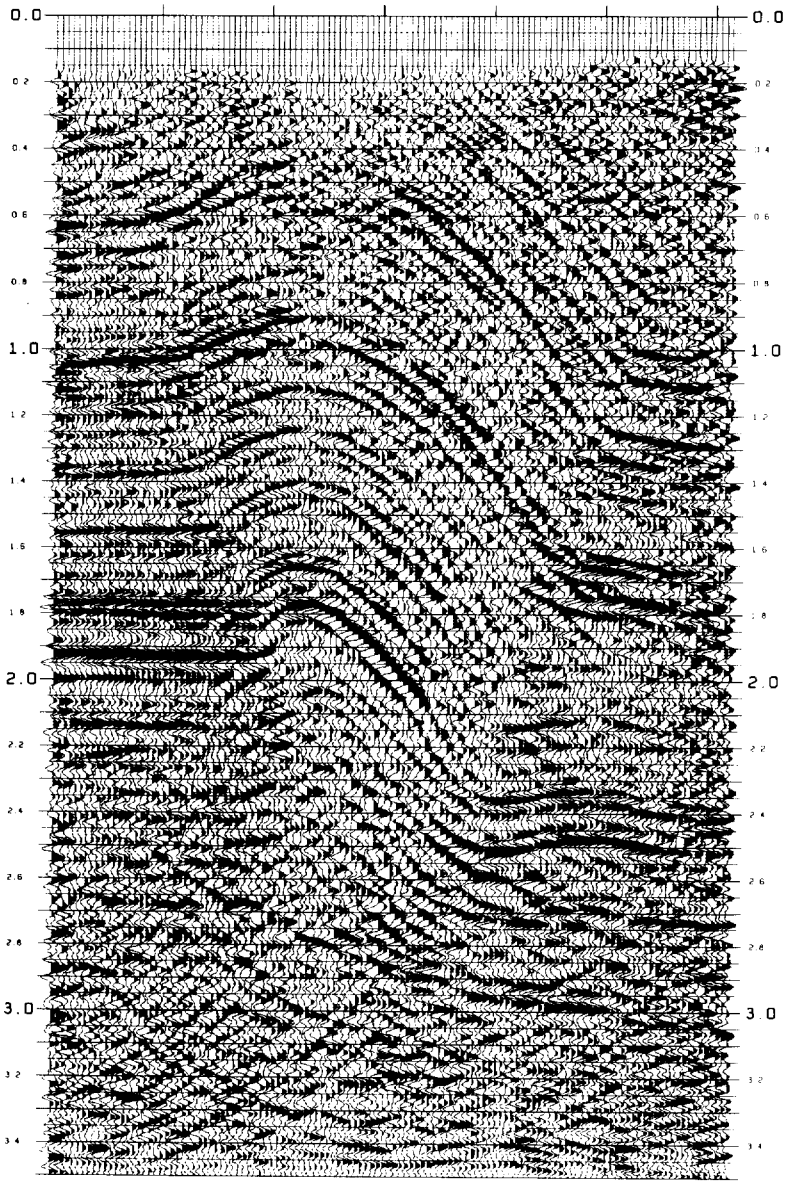

FIG. 23. A K-space migration of Figure 18.

where

$$W = \frac{c^2(X,Z)D^2}{\eta^2} + \frac{2d}{D}\left(1 - \frac{c^2(X'z)D^2}{\eta^2}\right). \quad (78)$$

Migration proceeds from the half-plane,

$$d = 0,\ D > 0, \quad (79)$$

to the half-plane,

$$d = D,\ D > 0. \quad (80)$$

All explicit dependence on X and Z now resides in the coefficient W of ϕ_{dd}. $W \neq 1$ reflects the fact that diffractions are not pure hyperbolas in a layered medium. Since ϕ_{dd} is ordinarily small, it is usually justifiable to replace W with an average constant value (usually a number between .5 and 1) for a given section. Then (77) has almost the form of equation

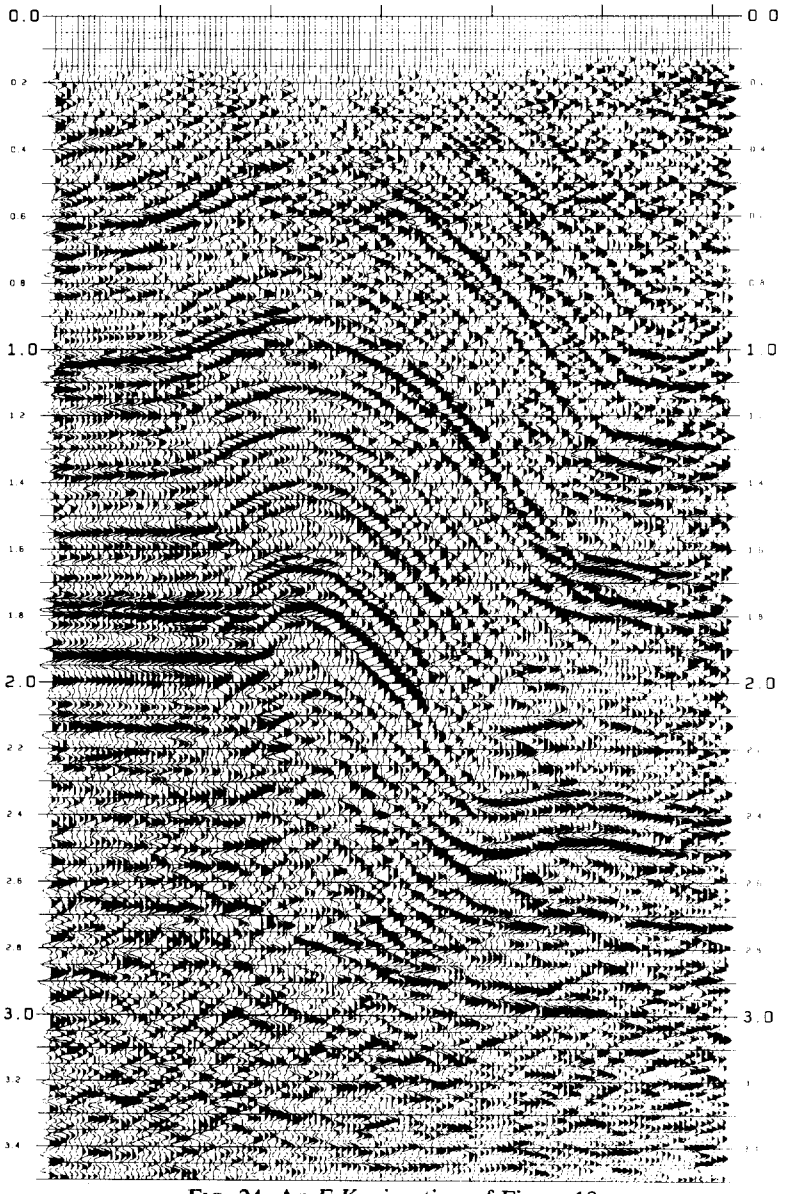

FIG. 24. An *F-K* migration of Figure 18.

(11), and the derivation of the *K*-space and *F-K* migration algorithms proceeds as outlined above, except for a slight modification of the dispersion relation (38) or (49).

Use of *K*-space or *F-K* migration in practice, then, involves a time to depth conversion (75). Even though simple to effect, this gives rise to practical difficulties in that (a) the frequency content of the data is altered; and (b) incorrect lateral velocity variations will distort the reflecting surfaces and cause improper migration. These problems can be lived with, however, and at present the *K*-space and *F-K* migration schemes appear to be practical and useful.

ACKNOWLEDGMENTS

I wish to thank the management of Continental Oil Co., for permission to publish this paper. Jerry Ware, Pierre Goupillaud, and Bill Heath have through

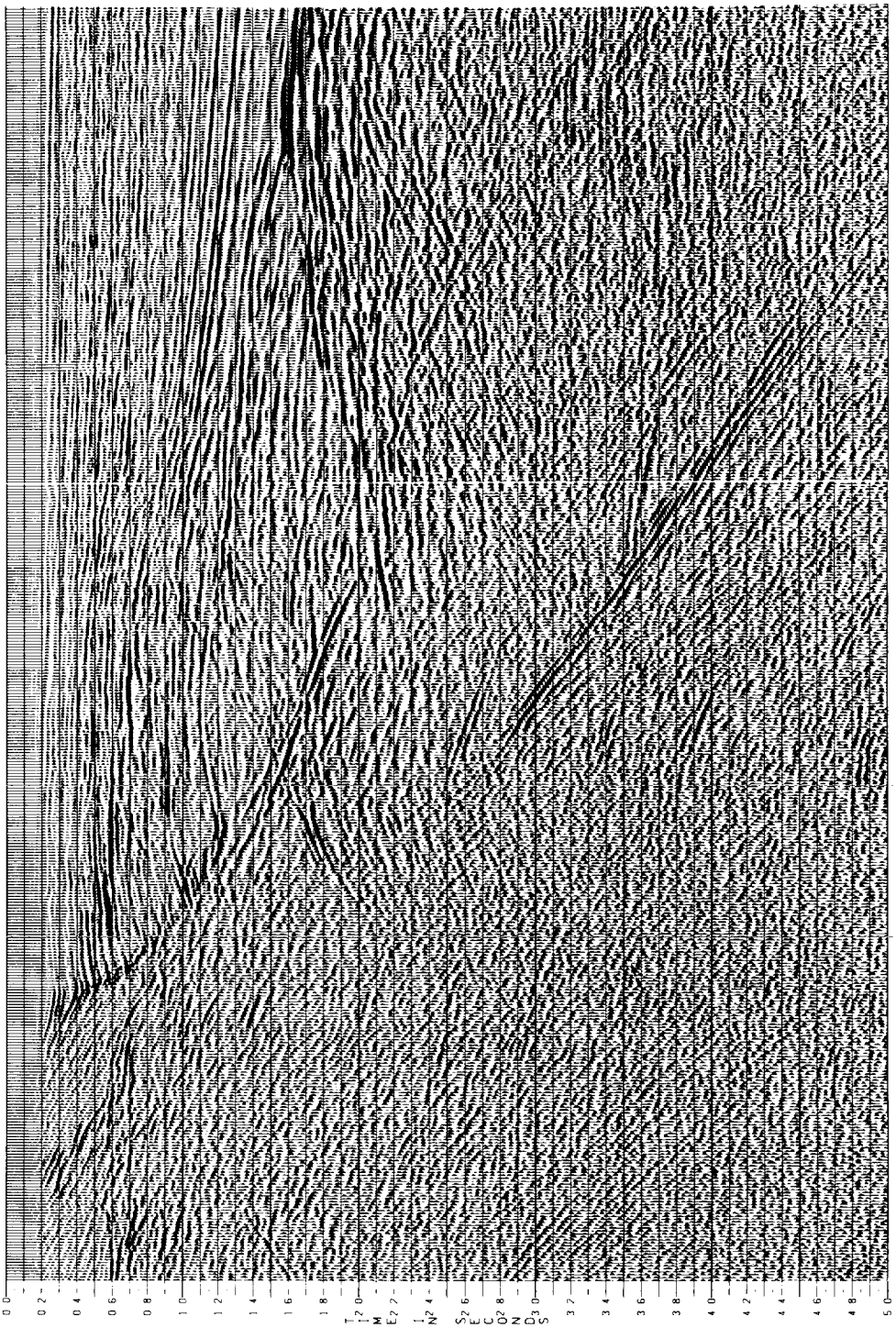

FIG. 25. A 24-fold stacked section.

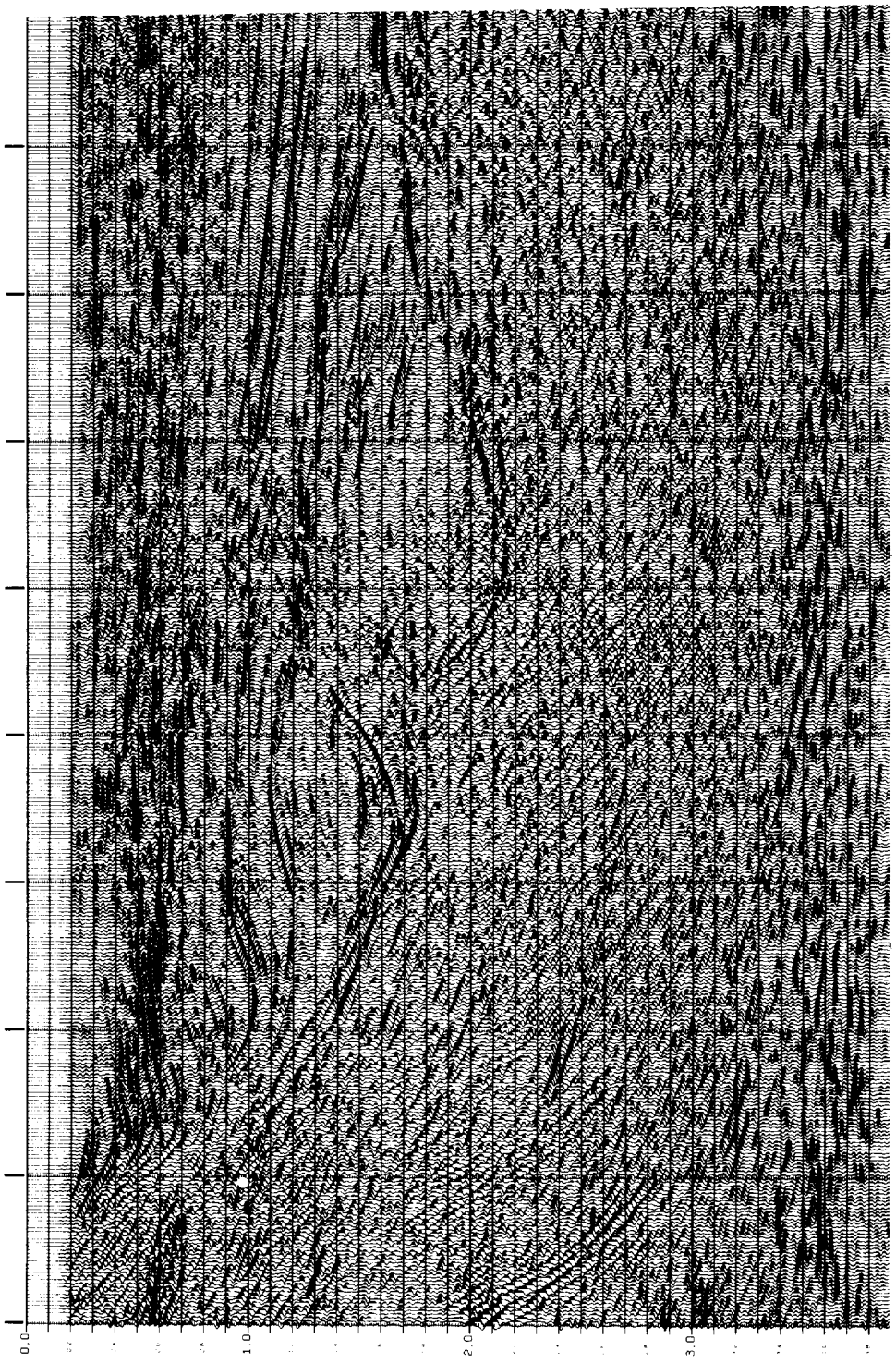

FIG. 26. An *F-K* migration.

several discussions contributed to the theoretical development of this work. Several staff members of the data processing division of Conoco's Exploration-Geophysics Department have, through discussion, criticism, and programming assistance, helped convert the theory to practice.

The development of the high-accuracy K-space migration scheme owes a great deal to the work of Bjorn Enquist at the Stanford Exploration Project. Francis Muir of Chevron has provided several helpful comments and suggestions in addition to the stability criteria and a more efficient form for the K-space algorithm. Of course, this paper would not have been possible but for the original inspiration of Jon Claerbout.

REFERENCES

Claerbout, J. F., 1971, Toward a unified theory of reflector mapping: Geophysics, v. 36, p. 467–481.

——— 1976, Fundamentals of geophysical data processing: New York, McGraw-Hill Book Co., Inc.

Claerbout, J. F., and Doherty, S. M., 1972, Downward continuation of moveout corrected seismograms: Geophysics, v. 37, p. 741–768.

French, W. S., 1974, Two-dimensional and three-dimensional migration of model-experiment reflection profiles: Geophysics, v. 39, p. 265–287.

——— 1975, Computer migration of oblique seismic reflection profiles: Geophysics, v. 40, p. 961–980.